Journal of Magnetism and Magnetic Materials 533 (2021) 167999

Contents lists available at ScienceDirect

Journal of Magnetism and Magnetic Materials

journal homepage: www.elsevier.com/locate/jmmm

Research articles

Magnetic vortex near the extended linear magnetic inhomogeneity

V.A. Orlov [a,b,*], G.S. Patrin [a,b,*], M.V. Dolgopolova [a,*], I.N. Orlova [c,*]

[a] Siberian Federal University, 79 Svobodny pr., Krasnoyarsk 660041, Russia
[b] Kirensky Institute of Physics Federal Research Center KSC Siberian Branch Russian Academy of Sciences, Akademgorodok 50, bld. 38, Krasnoyarsk 660036, Russia
[c] Krasnoyarsk State Pedagogical University named after V.P. Astafiev, 89 Ady Lebedevoi street, Krasnoyarsk 660049, Russia

ARTICLE INFO

Keywords:
Nanodot
Magnetic vortex
Magnetic inhomogeneity
Magnetic resonance
Thiel's equation
Skyrmions

ABSTRACT

In this paper, the problem of a magnetic vortex motion in a field of extended linear inhomogeneity is solved theoretically. The motion parameters are calculated by the method of collective variables (Thiel's equation) with the vortex effective mass and the third-order gyrovector. On the basis of the equation of motion, the influence of the core mass and the third-order gyrovector on the character of the vortex motion as a quasiparticle is analyzed. Using the method of magnetostatic charges, analytical expressions are obtained for the effective potentials where the vortex core is located: (a) near the edge of the magnet or at the boundary of different magnetic phases, (b) near the linear inhomogeneity of local anisotropy (bidirectional and unidirectional). The solution of the equation of motion made it possible to obtain the trajectories of the core in various physical situations. In addition, the paper discusses the features of the Hall effect for vortices/skyrmions, which are provided by the inertial properties and a third-order gyrovector. It is shown that when the core of a linear inhomogeneity crosses a unidirectional anisotropy or the boundary of magnetic phases, a curvature of the trajectory is observed, which is similar to the refraction of light at the boundary of optically dissimilar environment. It is important to note that the introduction of the mass and gyroscopic effect of the third order in the equation of motion showed that the motion of the vortex, even in a homogeneous potential, is not translational. In this case, the trajectory is an overlay of cycloids of different rotation frequencies (analytical expressions are obtained for the frequencies). It is shown that, the introduction of the mass and the gyroscopic term of the third order, the motion of the vortex core cannot be considered translational at least during the time of the transition mode until the stationary mode of motion takes place.

1. Introduction

The study of low-dimensional nanoscale magnets is paid much attention due to the prospects of developing of new-generation spintronics devices based on them (information carriers, sensors, logic elements, etc.). Various technological solutions for non-volatile memory devices are actively discussed in the literature. In the latter case, the main idea is bitwise information encoding on magnetic inhomogeneities of a special type, i. e. magnetic vortices and/or skyrmions. The logical "zero" or "one" can be set by the states of both the polarity and the chirality of the vortex magnetization [1–7].

One of the main difficulties in the development of working samples of devices is related to the reliability of the motion control of vortex structures in a magnet under the influence of fields, spin-polarized currents [8–10], gradient mechanical stresses [11,12] etc. The trajectory of such objects, even in simple models, can be extremely complex and often defies analytical description. Vortex formations move along intricate trajectories and exhibit unusual properties in the proximity of the defects in the magnetic structure. In such cases, computer modeling of the magnetization dynamics is useful [8,13–17].

In analytical calculations of the dynamic characteristics of the vortex magnetic structure, the method of collective variables in the hard vortex model proved to be productive. The backbone of the model is to neglect the distortion of the distribution function of the vortex magnetization in the process of its movement when approaching the inhomogeneity of the magnet or its edge. As shown in [18,19], such an approach is quite justified if the distance from the vortex core to the disturbing inhomogeneity significantly exceeds the size of the core, i.e. the central part of the vortex. The core of the vortex is a region with linear dimensions of the order of several nanometers, where the competition mainly of the exchange energy and the demagnetizing energy results in a strongly inhomogeneous distribution of magnetization with its exit from

* Corresponding authors.
E-mail address: vaorlov@sfu-kras.ru (V.A. Orlov).

https://doi.org/10.1016/j.jmmm.2021.167999
Received 2 January 2021; Received in revised form 29 March 2021; Accepted 4 April 2021
Available online 16 April 2021

the plane of the magnet.

In this case, the coordinate and the velocity of the center (the core) of the vortex are used as parameters that characterize the state of the vortex, and the distribution of magnetization inside the vortex is considered to be almost unchanged [20,21]. Subsequently, this approach was very successfully developed by many authors (see for example [22–26]). Within the approach, following the method proposed in [27] and developed in [28], the authors of the mentioned works obtained the equation of a magnetic vortex motion from Heisenberg model Hamiltonian as a quasiparticle in the form of:

$$\mathbf{G}_3 \times \ddot{\mathbf{v}} + \widehat{\mu}\dot{\mathbf{v}} + \mathbf{G} \times \mathbf{v} + \widehat{D}\mathbf{v} + \nabla W = 0. \tag{1}$$

Here the $\mathbf{G}$ and $\mathbf{G}_3$ coefficients are gyrovectors of the first and third order, respectively; [20,26,28], $\mathbf{v}$ is the core velocity; W is the potential energy possessed by the vortex, $\widehat{D}$ and $\widehat{\mu}$ are the tensors of effective coefficients of friction force and the effective mass of the vortex, respectively. The points above the vectors mean time differentiation. The x and y axes of the Cartesian coordinate system lie in the plane of the magnet. In a thin film (tape), gyrovectors have nonzero components only when they are perpendicular to the surface (z-components) [20,28]:

$$\begin{cases} \mathbf{G} = -\mathbf{e}_z \dfrac{M_S}{\gamma_g} \displaystyle\int_V \left[\frac{\partial m_z}{dx} \frac{\partial \varphi}{dy} - \frac{\partial m_z}{dy} \frac{\partial \varphi}{dx} \right] dxdydz, \\ \mathbf{G}_3 = -\mathbf{e}_z \dfrac{M_S}{\gamma_g} \displaystyle\int_V \left[\frac{\partial m_z}{dx} \frac{\partial \varphi}{d\dot{y}} - \frac{\partial m_z}{dy} \frac{\partial \varphi}{d\dot{x}} \right] dxdydz, \end{cases} \tag{2}$$

Where $\tan(\varphi) = m_x/m_y, m_x, m_y$ and m_z are the components of the unit magnetization vector, $\mathbf{e}_z$ is a unit vector of z-axis which is perpendicular to the plane of the magnet, γ_g is the gyromagnetic ratio, and M_S is the saturation magnetization. For the tensors components of a homogeneous isotropic environment [20,28]:

$$\widehat{D} = \begin{pmatrix} D_{xx} & 0 & 0 \\ 0 & D_{yy} & 0 \\ 0 & 0 & D_{zz} \end{pmatrix},$$

$$D_{xx} = D_{yy} = -\frac{\alpha M_S}{\gamma_g} \int_V \left[\frac{\partial m_z}{dx} \frac{\partial m_z}{dy} + \frac{\partial \varphi}{dy} \frac{\partial \varphi}{dx} \right] dxdydz, \tag{3}$$

$$\widehat{\mu} = \begin{pmatrix} \mu_{xx} & 0 & 0 \\ 0 & \mu_{yy} & 0 \\ 0 & 0 & \mu_{zz} \end{pmatrix},$$

$$\mu_{xx} = \mu_{yy} = \frac{M_S}{\gamma_g} \int_V \left[\frac{\partial m_z}{dx} \frac{\partial \varphi}{d\dot{y}} - \frac{\partial m_z}{d\dot{x}} \frac{\partial \varphi}{dy} \right] dxdydz. \tag{4}$$

The values of the D_{zz} and μ_{zz} components do not matter, since there is no motion of the core along the z axis in a thin magnet.

In most theoretical works, the authors do not pay attention to the first two terms of the left part (1). Often this is really justified. But in some physical situations, these terms result in interesting effects. For example, in [28–31] it is shown that the inertia in the vortex is responsible for the complex trajectory of the vortex in a two-dimensional potential, which is an overlap of cycloids. But it should be noted that often the mass was taken into account simultaneously with the neglect of energy dissipation during the motion of the core, at least in analytical estimates. At the same time, the dissipative term in (1) can have a noticeable effect on the character of the trajectory [32–34].

Special interest is currently focused on the study of the behavior of vortex magnetic objects near inhomogeneities of the magnetic structure. Inhomogeneities can be surface ones [35], fluctuations in the parameters of magnetic anisotropy [36,37] and external fields [38], boundaries between magnetic phases in composite magnets [39] etc. Indeed, in real materials, the cores of vortices (or skyrmions) are in the effective potential created not only by the edge of the magnets, but also by magnetic defects [40–42]. Often this potential is given by model functions, which is justified in most cases [43–45].

The influence of the potential of point defects in the magnetic structure can lead to interesting manifestations of the vortex structure properties. Depending on the nature of the defect, the core can be either captured by the defect field or scattered on it. The motion of the core may look as if the potential of a point defect has axial symmetry, but in fact it is not symmetric [46]. Moreover, the dissipation can significantly affect the nature of movement and equilibrium states. Interesting phenomena have been predicted in the computer simulation of linear defects, where the effects of refraction of the trajectory (like refraction of light) and acceleration of the vortex core are found (see, for example, the cycles of the authors' works [16,47]). But these studies did not include the core inertia and the third-order gyrovector. A particularly interesting and complex problem is the description of the motion of vortex cores in the field of multiple random defects, but due to the cumbersome nature of the equations, the authors still resort to preliminary study by numerical methods (see, for example, [48]).

In this paper, we present the analysis of Eq. (1) with the first two terms on the left side and the dissipative term (we discuss their role in the formation of the trajectory). The potential where the magnetic vortex moves is created by an extended linear defect. It is important to note that, as it is shown in [49], it is not necessary to limit the equation of motion (1) only to the inertial term, since in general the terms with $\widehat{\mu}\dot{\mathbf{v}}$ mass and $\mathbf{G}_3 \times \ddot{\mathbf{v}}$ gyrovector have the same order of smallness.

2. Effective potential of linear defects

Some cases of extended linear inhomogeneities of the magnetic characteristics of a planar magnet will be considered. We assume that the thickness of the h film (tape) is so small that the change in the magnetization in the direction perpendicular to the plane (along the z axis) can be ignored.

At the same time, the film thickness allows the vortex state to be realized in the xy [19] plane. We think that the magnet is isotropic in the xy plane and the position of the core is so far from the boundaries of the magnet that its displacement does not lead to any noticeable change in the magnetic energy, i.e., away from the defects, the core is considered to be in an indifferent equilibrium. In this case, the configuration of the magnetization in the vortex is determined only by the competition of the exchange energy and the demagnetizing energy. For estimation, the hard vortex model is used.

2.1. Linear boundary between phases with different magnetic parameters

Further we consider the model of a magnet divided into two magnetic phases by an extended rectilinear boundary. The phases are characterized by slightly different saturation magnetization. They are M_{S1} and M_{S2}, respectively. The differences between M_{S1} and M_{S2} must not be great for the hard vortex model to be fair.

An example of the configuration of such a magnet in the form of a tape with a vortex domain wall is shown in the Fig. 1. The magnetization in both phases of the tape is in the plane of the magnet, except for the central region of the vortex, i.e., the core. At the interface of the phases, which is indicated by a bold segment, magnetostatic charges arise, their interaction provides a change in the potential energy of the magnetic subsystem. The existence of magnetostatic charges is due to the difference between M_{S1} and M_{S2}. The charge density is given by the function $\sigma(y)$. Depending on the direction of the magnetization in the sections of the "skirt" of the vortex crossing the boundary, the $\sigma(y)$ function can take either a positive or a negative value.

Fig. 2 shows the geometry of the problem of calculating the energy of a magnetic vortex depending on the distance from the core to the linear inhomogeneity. The following notation is introduced: δ is a characteristic size of the vortex, ds_1 and ds_2 are elementary sites, the interaction between them will be calculated.

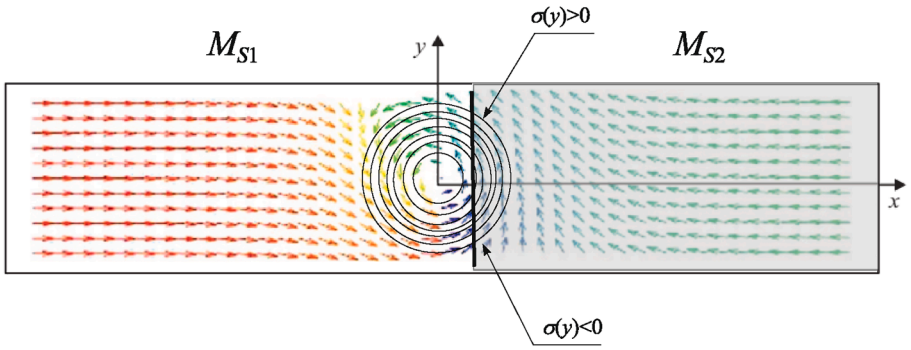

Fig. 1. The model of interaction between the magnetization of a vortex (vortex domain wall) and inhomogeneity in the form of a jump in magnetic parameters.

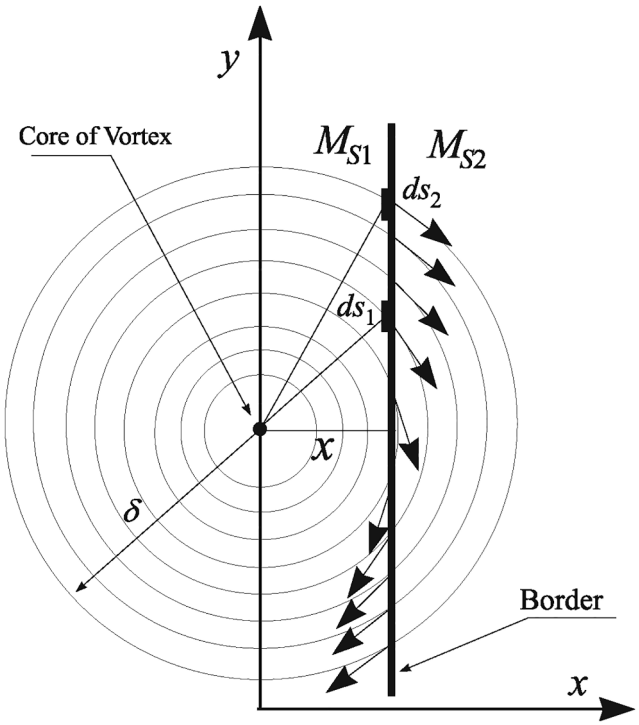

Fig. 2. The mechanism of magnetostatic charges occurrence at the interface.

The interaction energy of elementary sites can be written as:

$$dW_m = \frac{\mu_0}{4\pi}\frac{\sigma(y_1)\sigma(y_2)}{|y_2 - y_1|}ds_1 ds_2. \tag{5}$$

The surface density of magnetostatic charges is determined by the perpendicular magnetization components at the phase boundary: $\sigma(y) = m_{xy}(x,y)(M_{S1} - M_{S2})y/\sqrt{x^2+y^2}$, $m_{xy}(x,y) = \sqrt{1-m_z^2(x,y)}$ is a projection of the unit magnetization vector on the xy plane (see Fig. 2). Then for energy (5) we can write:

$$dW_m = \frac{\mu_0}{4\pi}\frac{h^2 m_{xy}(x,y_1)m_{xy}(x,y_2)(M_{S1}-M_{S2})^2 y_1 y_2}{\sqrt{(x^2+y_1^2)(x^2+y_2^2)(y_1-y_2)^2}}dy_1 dy_2. \tag{6}$$

The linear size of the vortex core $\delta_0 \approx \sqrt{A/M_S}$ (A is an exchange constant) is of the ~ 10 nm, order, which is much smaller than the size of a "skirt" of the δ vortex. It means that $m_z = 0$ can be considered almost on the entire area of the vortex wall (this condition is not met for certain types of skyrmions). In addition, it can be assumed approximately that the vortex has a relatively sharp boundary, i.e., the magnetization is almost uniform outside of it. It is natural to think that the error associated with this approximation is small in the case when the vortex core is located relatively close to the inhomogeneity, and, on the contrary, can have a value at distances to the defect comparable to δ.

For the total potential energy, we write:

$$W_m = \frac{\mu_0}{4\pi}h^2\delta(M_{S1}-M_{S2})^2 I(\rho). \tag{7}$$

where $\rho = x/\delta, I(\rho)$ is a dimensionless integral defined by the expression:

$$\begin{cases} I(\rho) = \frac{1}{2}\int_{-\sqrt{1-\rho^2}}^{\sqrt{1-\rho^2}}\int_{-\sqrt{1-\rho^2}}^{\sqrt{1-\rho^2}}\frac{Y_1 Y_2}{\sqrt{(\rho^2+Y_1^2)(\rho^2+Y_2^2)(Y_1-Y_2)^2}}dY_1 dY_2, & \rho < 1, \\ 0, & \rho \geqslant 1. \end{cases} \tag{8}$$

where $Y = y/\delta$. It is difficult to calculate analytically the expression (8) but the result is well approximated by a function of the form (see Fig. 3):

$$I(\rho) \approx 3.4\left(e^{2(1-\rho)} - 1\right). \tag{9}$$

Together with (7) for the x-component of the vortex interaction force with inhomogeneity at $\rho < 1$, we can write:

$$f_x\left(\rho\right) = -\frac{dW_m}{dx} = \frac{\mu_0}{4\pi}h^2(M_{S1}-M_{S2})^2\frac{dI(\rho)}{d\rho} \approx 1.7\frac{\mu_0}{\pi}h^2(M_{S1}-M_{S2})^2 e^{2(1-\rho)}. \tag{10}$$

2.2. The linear inhomogeneity of the magnetic anisotropy

Next, we consider the effective interaction of a magnetic vortex core with a rectilinear anisotropic inhomogeneity in the form of a thin

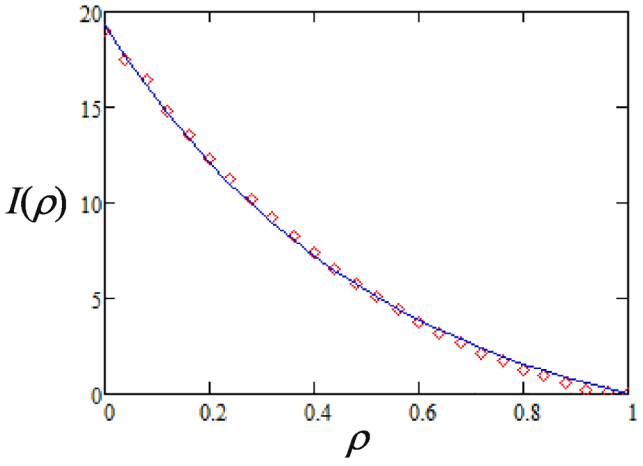

Fig. 3. The result of numerical calculation of the integral (8) (circles) in comparison with the fitting function (9) (a solid curve).

filament with the direction of the light axis different from the rest of the magnet. As the distance between the core and the filament changes, the energy of the magnetic system changes, as well. This variation is due to a change in the magnetic anisotropy energy of the magnetization parts on the defect. The calculation of this energy is carried out by summing the anisotropy energy of small sections, which the linear inhomogeneity is divided into (see 4).

The anisotropy energy of the elementary volume is written as:

$$dW_a = -K(\mathbf{ml})^2 dV. \tag{11}$$

where K is the magnetic anisotropy constant of the defect, $\mathbf{m}$ and $\mathbf{l}$ are the unit vectors of the magnetization direction and the light anisotropy axis, respectively, $dV = hbdy$ is the elementary volume, and b is the thickness of the inhomogeneity. For the calculations simplicity, but without loss of a general view, it can be considered that the anisotropy axis (LAA) of the filamentary defect is located in the plane formed by the filament itself and normal to the surface of the magnet. The direction of the LAA is given by the α angle, which is measured in this plane from the filament. The scalar product of vectors can be represented as:

$$\mathbf{ml} = m_x l_x + m_y l_y + m_z l_z = q\sqrt{1-m_z^2}\cos\left(\xi\right)\cos\left(\alpha\right) + p\left|m_z\right|\sin\left(\alpha\right). \tag{12}$$

Where ξ is the angle between the magnetization of the elementary volume and the filament (see Fig. 4), $q = \pm 1$ is the vortex chirality, the sign which is determined by the direction of the magnetization twist: clockwise or anticlockwise, $p = \pm 1$ is the polarity of the core magnetization. The sign of polarity is positive when the direction of magnetization in the center of the core coincides with the direction of the $\mathbf{e}_z$ unit vector and vice versa.

For the total anisotropy energy, we have:

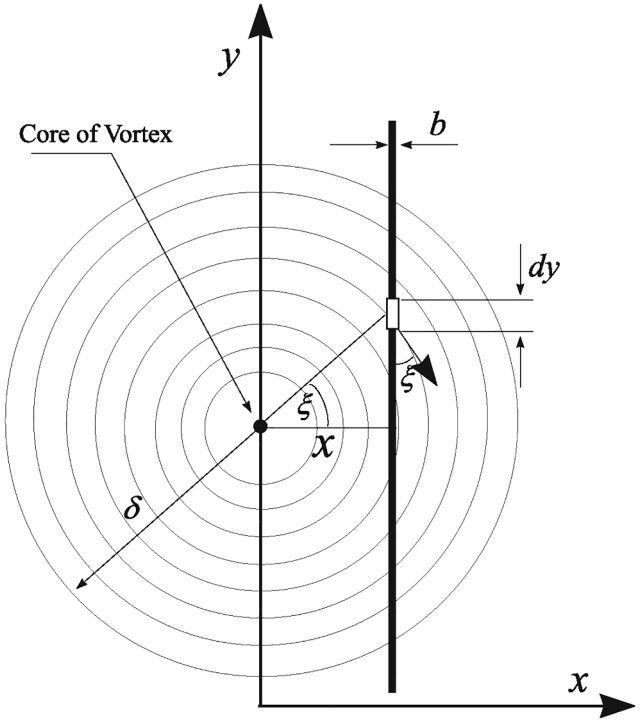

Fig. 4. The model of the vortex interaction with an anisotropic linear defect.

$$\begin{aligned} W_a &= -Khb\int_{-\sqrt{\delta^2-x^2}}^{\sqrt{\delta^2-x^2}} (\mathbf{ml})^2 dy \\ &= -Khb\int_{-\sqrt{\delta^2-x^2}}^{\sqrt{\delta^2-x^2}} \left[q\sqrt{1-m_z^2}\cos\left(\xi\right)\cos\left(\alpha\right) + p\left|m_z\right|\sin\left(\alpha\right)\right]^2 dy. \end{aligned} \tag{13}$$

Using the dimensionless parameters introduced earlier, and taking into account that $\cos(\xi) = x/\sqrt{x^2+y^2}$, we get:

$$W_a = -Khb\delta\int_{-\sqrt{1-\rho^2}}^{\sqrt{1-\rho^2}} \left[q\rho\cos\left(\alpha\right)\sqrt{\frac{1-m_z^2}{\rho^2+Y^2}} + p\left|m_z\right|\sin\left(\alpha\right)\right]^2 dY. \tag{14}$$

For the final calculation of the integral, it is necessary to have a functional dependence of the magnetization distribution in the $m_z(x,y)$ vortex. Various model dependences based on the solution of the static Landau-Lipschitz equation are proposed in the literature. But with all the diversity, it is important that these functions are localized in a small region of space of the core size order. It allows to make an approximate expression for (14) if the vortex core does not creep over the filamentous inhomogeneity. In this case, the z-component of the magnetization can be considered small $|m_z| \ll 1$. Then for $\alpha \neq \pi/2$ and $\rho < 1$ it can be written:

$$W_a = -Khb\delta\rho^2\cos^2\left(\alpha\right)\int_{-\sqrt{1-\rho^2}}^{\sqrt{1-\rho^2}} \frac{dY}{\rho^2+Y^2} = -2Khb\delta\cos^2\left(\alpha\right)I_a\left(\rho\right), \tag{15}$$

where

$$I_a\left(\rho\right) = \rho\arctan\left(\frac{\sqrt{1-\rho^2}}{\rho}\right). \tag{16}$$

In this case, the equilibrium distance between the core and the ρ_{eq} filament is determined by the simple condition $\frac{dW_a}{d\rho} = 0$. The numerical calculation shows $\rho_{eq} \approx \pm 0.652$. It means that the vortex can potentially be captured by a filamentous defect and held at the ρ_{eq} distance.

When $\alpha \approx \pi/2$ or the core is located close to the defect, the second term in square brackets of expression (14). plays the main role. Often, the $m_z(\rho, Y) = p\exp\left(-\frac{\rho^2+Y^2}{(\delta_0/\delta)^2}\right)$ ansats is chosen as the function that sets the magnetization profile. In this case, the energy takes the form:

$$\begin{aligned} W_a &= -Khb\delta\sin^2\left(\alpha\right)\int_{-\sqrt{1-\rho^2}}^{\sqrt{1-\rho^2}} m_z^2(\rho, Y)dY \\ &= -\frac{\pi}{2}Khb\delta_0\sin^2\left(\alpha\right)\exp\left(-\frac{2\rho^2}{(\delta_0/\delta)^2}\right)\mathrm{Erf}\left(\frac{\sqrt{2(1-\rho^2)}}{\delta_0/\delta}\right). \end{aligned} \tag{17}$$

The minimum of the function is realized at $\rho_{eq} = 0$, which also means that the core can be captured, but the equilibrium will be achieved when the center of the vortex is located directly on the inhomogeneity. The form of dependence of the $W_a(\rho, \alpha)$ dimensionless part in the general case according to the results of numerical calculations is shown in Fig. 5.

The asymmetry of the potential energy with respect to the position of the vortex near the inhomogeneity is paid attention. According to the expression (14) it can be concluded that the value of the subintegral expression depends on the sign of the $\pi_T = qp$ product, which was not observed for the energy considered in paragraph (a) of this section.

The dependence of the potential energy on the sign of π_T allows to consider that vortices with different values of the product of polarity and chirality in the field of such a defect will move along different trajectories. The sign of the qp product for the interaction energy of the core with inhomogeneity does not matter only in the $\alpha = 0, \pi/2$ limiting cases.

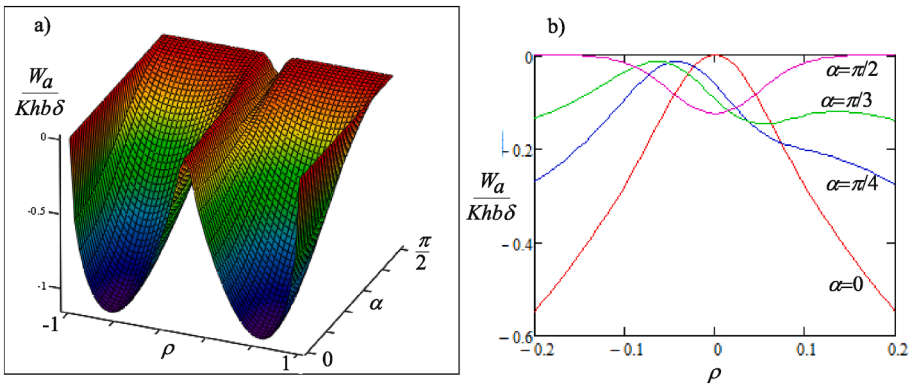

Fig. 5. The dimensionless part of the dependence of the interaction energy of the vortex with the filamentous inhomogeneity of the anisotropy on the distance between the core and the defect and on the LAA angle (Fig. (a)). Figure (b) is the dependence on the distance between the core and the inhomogeneity for some values of the α angle in the range of small ρ in the vicinity of the defect. The constructions are made for the case $\delta_0/\delta = 0.01$, $qp = 1$.

The case when the inhomogeneity of magnetic anisotropy has not bidirectional, but unidirectional symmetry is of great interest. Such a phenomenon can be observed, for example, at the junction of ferro-and antiferromagnetic phases. The energy of the core in the field of such inhomogeneity is represented as:

$$W_a = -Khb\int_{-\sqrt{\delta^2-x^2}}^{\sqrt{\delta^2-x^2}} \mathbf{ml}dy = -Khb\delta\int_{-\sqrt{1-\rho^2}}^{\sqrt{1-\rho^2}}\left[q\rho\cos(\alpha)\sqrt{\frac{1-m_z^2}{\rho^2+Y^2}}+p|m_z|\sin(\alpha)\right]dY. \quad (18)$$

In the $\alpha \approx \pi/2$ or $|m_z| \approx 1$ limiting case, the expression for energy (18) takes the form:

$$W_a \approx -pKhb\delta\sin(\alpha)\int_{-\sqrt{1-\rho^2}}^{\sqrt{1-\rho^2}}|m_z|dY = -pKhb\delta_0\sqrt{\pi}\sin(\alpha)\exp\left(-\frac{\rho^2}{(\delta_0/\delta)^2}\right)\mathrm{Erf}\left(\frac{\sqrt{1-\rho^2}}{\delta_0/\delta}\right). \quad (19)$$

In the $\alpha \to 0$ or $|m_z| \to 0$ limiting case, the energy takes the form:

$$W_a \approx -qKhb\delta\cos(\alpha)\int_{-\sqrt{1-\rho^2}}^{\sqrt{1-\rho^2}}\frac{\rho dY}{\sqrt{\rho^2+Y^2}} = -qKhb\delta\cos(\alpha)\rho\ln\left(\frac{1+\sqrt{1-\rho^2}}{1-\sqrt{1-\rho^2}}\right). \quad (20)$$

Fig. 6 shows the shape of the potential generated by a linear inhomogeneity with uniaxial unidirectional anisotropy.

In this case, unlike bidirectional anisotropy, the behavior of the core will be affected not by the product of the p and q parameters, but by the values of each of them separately. Indeed, vortices with different combinations of $\{p,q\}:\{1,1\},\{1,-1\},\{-1,1\}$ and $\{-1,-1\}$, will have different potential energies in the field of inhomogeneity, therefore, they will move under the action of different forces and along different trajectories. In future it will allow devices to organize the sorting of vortex flows (skyrmions) based on different polarities and chiralities (skyrmion Hall effect).

In conclusion of this section, we note that the energies considered in both point (a) and point (b) in a small neighborhood near the equilibrium position of the core are approximated by quadratic functions of the x coordinate. This circumstance makes it possible to make simple analytical calculations of the nature of the core motion based on the linear equation of motion at least for small amplitudes of the core displacement.

3. Vortex motion in the linear defect potential

Further we consider the features of the trajectory of the magnetic vortex core in the potential created by linear inhomogeneity, with and without the various terms in the left part of Eq. (1). The general thing in this case is the dependence of the potential energy of the core on only one spatial x coordinate. First of all, the preliminary transformations of the equation of motion are performed and it is rewritten in projections on the Cartesian coordinate system.

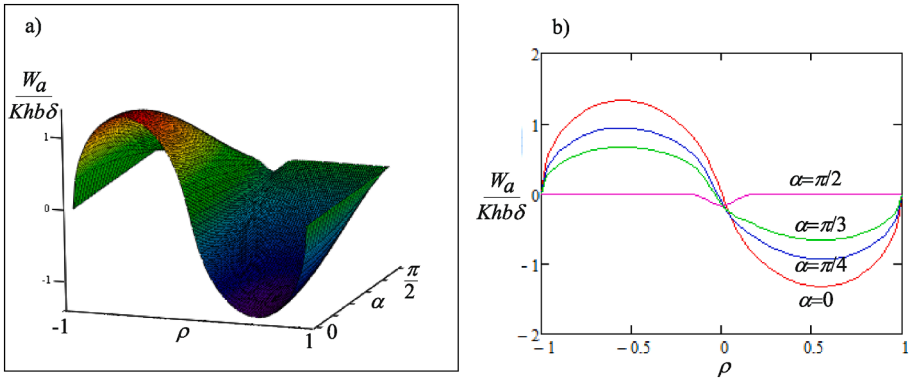

Fig. 6. The dimensionless part of the dependence of the interaction energy of the vortex with the filamentous inhomogeneity of unidirectional anisotropy on the distance between the core and the defect and on the LAA angle (Fig. (a)). Fig. (b) is the dependence on the distance between the core and the inhomogeneity for some values of the α angle. The constructions are made for the $\delta_0/\delta = 0.01$, $q = p = 1$ case.

$$\begin{aligned}&\mathbf{G}_3\times\ddot{\mathbf{v}}=-\mathbf{e}_x G_3\ddot{v}_y+\mathbf{e}_y G_3\ddot{v}_x,\\&\mathbf{G}\times\mathbf{v}=-\mathbf{e}_x Gv_y+\mathbf{e}_y Gv_x,\\&\widehat{\mu}\dot{\mathbf{v}}=\mathbf{e}_x\mu\dot{v}_x+\mathbf{e}_y\mu\dot{v}_y,\\&\widehat{D}\mathbf{v}=\mathbf{e}_x Dv_x+\mathbf{e}_y Dv_y,\\&\nabla W=-\mathbf{e}_x f_x-\mathbf{e}_y f_y,\end{aligned}\tag{21}$$

where $f_x=-\frac{\partial W}{\partial x}, f_y=-\frac{\partial W}{\partial y}$ – x- and y are components of the force acting on the core, $\mathbf{e}_x$ and $\mathbf{e}_y$ are unit vectors of the Cartesian coordinate system.

Together with (21), the equation of motion can be represented as:

$$\begin{cases}-G_3\ddot{v}_y+\mu\dot{v}_x-Gv_y+Dv_x-f_x=0,\\G_3\ddot{v}_x+\mu\dot{v}_y+Gv_x+Dv_y-f_y=0.\end{cases}\tag{22}$$

Further some interesting and practically significant special cases of the solution of the system (22) are given.

3.1. The case of a homogeneous magnet without external influences

In this case, the forces are equal to zero: $f_x=f_y=0$ in the system of Eqs. (22). The type of equations suggests that trial solutions should be found in the form:

$$\begin{cases}v_x=v_{0x}\exp(-(i\omega+\lambda)t),\\v_y=iv_{0y}\exp(-(i\omega+\lambda)t).\end{cases}\tag{23}$$

Where $i=\sqrt{-1}$ is an imaginary unit. After the solutions (23) are substituted into Eqs. (22), a system of algebraic equations for complex velocity amplitudes is obtained:

$$\begin{cases}v_{0x}(-\mu(i\omega+\lambda)+D)-v_{0y}\left(iG_3(i\omega+\lambda)^2+iG\right)=0,\\v_{0x}\left(G_3(i\omega+\lambda)^2+G\right)-v_{0y}(i\mu(i\omega+\lambda)-iD)=0.\end{cases}\tag{24}$$

After is equated to zero the determinant of the matrix constructed on the v_x, v_y coefficients, the equation for ω and λ is obtained:

$$\omega_{1,2}=\pm\frac{1}{2}\Omega_3\left(1-\sqrt{1+4\frac{\Omega_1}{\Omega_3}+4\frac{\lambda^2}{\Omega_3^2}}\right),\tag{25}$$

$$\lambda=\frac{\Omega_3}{2\sqrt{2}}\left[-1-4\frac{\Omega_1}{\Omega_3}+\sqrt{\left(1+4\frac{\Omega_1}{\Omega_3}\right)^2+16\frac{\Lambda^2}{\Omega_3^2}}\right]^{\frac{1}{2}}.\tag{26}$$

Here the notation is introduced: $\Lambda=D/\mu, \Omega_1=G/\mu, \Omega_3=\mu/G_3$.

In the case of weak damping ($D\to 0$) for the trajectory parameters, we obtain:

$$\begin{cases}\lambda\approx\dfrac{\Lambda}{\sqrt{1+4\frac{\Omega_1}{\Omega_3}}},\\\omega_{1,2}\approx\dfrac{\Omega_3}{2}\left[\pm 1+\left(\sqrt{\left(1+4\frac{\Omega_1}{\Omega_3}\right)}+\dfrac{4\Lambda^2/\Omega_3^2}{(1+4(\Omega_1/\Omega_3))^{\frac{3}{2}}}\right)\right].\end{cases}\tag{27}$$

In the general case, the solution of the motion equation is represented by a superposition of modes with the $v_0^{(1)}, v_0^{(2)}$ corresponding fractions:

$$\begin{cases}v_x=v_0^{(1)}\exp(-(i\omega_1+\lambda)t)+v_0^{(2)}\exp(-(i\omega_2+\lambda)t),\\v_y=iv_0^{(1)}\exp(-(i\omega_1+\lambda)t)+iv_0^{(2)}\exp(-(i\omega_2+\lambda)t).\end{cases}\tag{28}$$

In fact, we have a frequency doublet with the $\Delta\omega=\omega_1-\omega_2=2|\omega_{1,2}|$ splitting value.

In the limit at $D\to 0$, the expression for harmonic frequencies (25) takes the form:

$$\omega_{1,2}=\frac{\Omega_3}{2}\left[\pm 1+\sqrt{1+4\frac{\Omega_1}{\Omega_3}}\right],\tag{29}$$

which has been presented and discussed earlier in [28,49]. In the particular case of $G_3\to 0$ ($\Omega_3\to\infty$), the expressions for the frequencies of modes (25) take the form:

$$\omega_{1,2}=\pm\Omega_1=\pm\frac{G}{\mu}.\tag{30}$$

A spectrum similar to (30) has been obtained and discussed by various authors in models with the presence of a potential restoring force [22,25,29,30,50,51] and was observed experimentally (see [52–54] for example). It is remarkable that even without returning forces (homogeneous potential), the trajectory is not rectilinear and has a quasi-periodic character. This circumstance gives a potential opportunity to determine some characteristics of the vortex structure in the ferromagnetic resonance experiment.

Analytical calculations of the G_3 and μ coefficients included in the (1) equation have been obtained in [25]: $G_3\approx\delta/(4\pi M_S\gamma^3)$ (the value of δ can be interpreted as the characteristic linear size of the vortex), $\mu\approx h/\gamma^2$. The expressions for the G and D parameters are well known and are used for the case of the exponential distribution of the z – magnetization component in a vortex in a thin magnet (see for example [55–57]): $G=2\pi M_S h/\gamma, D=\alpha_d\pi M_S h\left(2+\ln\left(\frac{\delta}{\delta_0}\right)\right)\Big/\gamma$, where α_d is the damping parameter of the ferromagnetic material. Numerical estimates of the coefficients for popular magnetic materials are in the ranges: $\mu\sim 10^{-22}-10^{-24}\mathrm{kg}, G\sim 10^{-12}-10^{-14}\mathrm{Js/m^2}$ [30,58,59], $G_3\sim 10^{-36}\mathrm{Js^3/m^2}$ [60]. The data show that the values of the Ω_1, Ω_3 parameters, and therefore $\omega_{1,2}$ are on the order of ten gigahertz, which significantly exceeds the frequency of the gyrotropic mode, which is hundreds of megahertz.

In addition, the inertial term in the equation of motion allowed to interpret the results of experimental measurement of the skyrmion mass [61] and its role in the magnetization dynamics [62].

3.2. Magnetic vortex in a potential varying according to a linear law

In this section, the motion of the vortex core in a potential that satisfies the condition $\nabla W=const\neq 0$ is considered. It means the core moves under the action of projections of f_{0x} and f_{0y} forces, which do not depend on coordinates and time. This situation can be realized in planar magnets in the case of vortex motion caused by the spin-polarized currents (see for example [12]), mechanical stress gradients and/or anisotropy fields [11,12,36], magnetic fields [16], etc.

The equations of motion when there are constant forces take a simple form after replacing the variables according to the scheme:

$$\begin{cases}v_x=u_x+\dfrac{f_{0x}D+f_{0y}G}{G^2+D^2},\\v_y=u_y+\dfrac{f_{0y}D-f_{0x}G}{G^2+D^2}.\end{cases}\tag{31}$$

With such substitution, the system of Eqs. (22) takes the form:

$$\left\{-G_3\ddot{u}_y+\mu\dot{u}_x-Gu_y+Du_x=0,\quad G_3\ddot{u}_x+\mu\dot{u}_y+Gu_x+Du_y=0.\right.\tag{32}$$

The solution of this system does not differ from the procedure which has already been described in the previous paragraph. The expressions for harmonic frequencies and the damping parameter do not differ from expressions (25) and (26),respectively, but the trajectories have features due to the drift with constant speed projections given by additions in the right-hand parts of expressions (31):

$$\begin{cases} v_x = v_0^{(1)}\exp(-(i\omega_1+\lambda)t) + v_0^{(2)}\exp(-(i\omega_2+\lambda)t) + \dfrac{f_{0x}D + f_{0y}G}{G^2+D^2}, \\ v_y = iv_0^{(1)}\exp(-(i\omega_1+\lambda)t) + iv_0^{(2)}\exp(-(i\omega_2+\lambda)t) + \dfrac{f_{0y}D - f_{0x}G}{G^2+D^2}. \end{cases} \quad (33)$$

It should be noted that the nature of the core explains its trend to drift in a direction perpendicular to the applied force and makes oscillations. But not in the case of noticeable dissipation. Indeed, the last terms in the right-hand sides of expressions (33) indicate the uniform drift along both the x and y axes, even if only one of the force components (f_{0x} or f_{0y}) is present. Drift in the strictly perpendicular direction of the applied constant force is possible only at $D = 0$ ($D \ll G$). When there is a noticeable dissipation, the drift displacement of the core occurs at an acute angle to the direction of the applied force. After a stationary motion is established (in a time $\tau \gg 1/\lambda$), the core moves in the direction determined by the angle measured from the y-axes:

$$\tan(\varphi) = \frac{f_{0x}D + f_{0y}G}{f_{0y}D - f_{0x}G}, \quad (34)$$

and the angular rates are determined by the expression (25).

An approximate view of the trajectories of the magnetic vortex core for this case is shown in Fig. 7, which shows how the direction of the drift motion of the core changes at different values of the λ damping parameter and $f_x = 0$. If $D \neq 0$ the sum of the force $\mathbf{F} = -\nabla W$ and the dissipation force $\mathbf{F}_{dis} = -D\mathbf{v}$ is not directed parallel to the y-axis. This explains the existence of $v_y \neq 0$. In the stationary regime, after the damping of oscillations, the direction of drift of the vortex core is set by a compromise between the forces $\mathbf{F}, \mathbf{F}_{dis}$ and the gyroscopic force $\mathbf{G} \times \mathbf{v}$.

3.3. Magnetic vortex in the potential of linear inhomogeneity

Further, the motion of the vortex core in the potential created by a linear defect is considered. The inhomogeneity is located along the y-axis in the coordinate system chosen by us. In this case, the potential

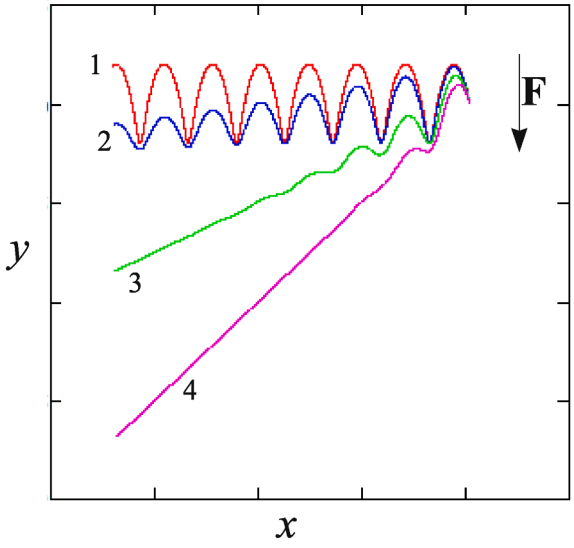

Fig. 7. The typical trajectories of the vortex core motion under the influence of a constant force. The curves are constructed under the same initial conditions. Based on the numerical data on the coefficients of the (1) equation, we established the $\Omega_1/\Omega_3 = 10$ ratio for constructing the curves. Then from (25) and (26) we can write: $\lambda/\Omega_3 \approx 6.4\alpha_d$, $\omega_{1,2}/\Omega_3 \approx \pm(2.7 + 1.6\alpha_d^2)$. The arrow shows the direction of the constant force $\mathbf{F} = -\nabla W$ acting on the vortex core. The curves are constructed at the following values of the damping parameter: 1 – $\alpha_d = 0$, 2 – $\alpha_d = 0.01$, 3 – $\alpha_d = 0.05$, 4 – $\alpha_d = 0.1$.

energy of the core depends only on the x coordinate. If the core shifts slightly from the equilibrium position, the $W(x) \approx \kappa x^2/2$ quadratic dependence can be suggested. Where κ is the effective stiffness coefficient of the core-inhomogeneity coupling, which depends on the nature of the inhomogeneity.

Table 1 shows the values of the κ coefficients for the types of inhomogeneities considered in Section 2 of this article. The coefficients are obtained by decomposing the energy by degrees of smallness of the core position deviation from the ρ_0 equilibrium to the second-order term.

The peculiarity of the potential created by the jump of magnetic parameters (point (a) from Section 2) should be noted. At any distance from the core to the boundary, this inhomogeneity creates a potential that provides repulsion of the vortex. Therefore, the equilibrium position in this case is achievable only if there is an additional force competing with the force created by the defect. For example, it can be the F_x, force created by the included magnetic field, the currents, etc. Then, with the expression (10), we get: $f_x = 1.7\frac{\mu_0}{\pi}h^2(M_{S1} - M_{S2})^2 e^{2(1-\rho)} - F_x$. Hence, for the equilibrium position of the core ($f_x = 0$), we get: $\rho_0 = 1 + \ln\left(1.7\mu_0 h^2(M_{S1} - M_{S2})^2/(\pi F_x)\right)$.

The trajectory of the core in this case is described by a system of equations:

$$\begin{cases} -G_3\ddot{v}_y + \mu\dot{v}_x - Gv_y + Dv_x - f_{0x} + \kappa x = 0, \\ G_3\ddot{v}_x + \mu\dot{v}_y + Gv_x + Dv_y - f_{0y} = 0. \end{cases} \quad (35)$$

where f_{0x} and f_{0y} – x and y are the components of the constant force applied to the core. The nature of the terms of these equations suggests that the functions should be chosen as trial solutions:

$$\begin{cases} x(t) = x_0 + v_{0x}t + a_x\exp(-(i\omega+\lambda)), \\ y(t) = v_{0y}t + ia_y\exp(-(i\omega+\lambda)). \end{cases} \quad (36)$$

where a_x and a_y are constant values-complex amplitudes. Indeed, due to the potential well in the yz section, there is an equilibrium position $x_0 = \rho_0\delta$. Due to the constant components of the f_x and f_y forces, it is reasonable to expect drift displacement with the v_{0x} and v_{0y}rates. The terms proportional to the first powers of speed and derivatives of speed suggest solutions in the form of exponents with both real and imaginary arguments.

Substituting the trial solutions (36) into the system (35) and grouping the terms gives the following equations for the parameters of the trial solutions:

$$\begin{cases} iG_3a_y(i\omega+\lambda)^3 + \mu a_x(i\omega+\lambda)^2 + iGa_y(i\omega+\lambda) - Da_x(i\omega+\lambda) + \kappa a_x = 0, \\ -G_3a_x(i\omega+\lambda)^3 + i\mu a_y(i\omega+\lambda)^2 - Ga_x(i\omega+\lambda) - iDa_y(i\omega+\lambda) = 0, \end{cases} \quad (37)$$

$$\begin{cases} -Gv_{0y} + Dv_{0x} - \kappa x_0 - f_{0x} = 0, \\ Gv_{0x} + Dv_{0y} - f_{0y} = 0, \\ v_{0x} = 0. \end{cases} \quad (38)$$

From system (38), it follows:

$$\begin{cases} v_{0y} = \dfrac{f_{0x}}{D}, \\ x_0 = \dfrac{f_{0x}D + f_{0y}G}{\kappa D}. \end{cases} \quad (39)$$

After the determinant of the matrix constructed on the coefficients at a_x and a_y from (37) is equated to zero, we obtain the equation for frequencies and the damping parameter:

$$\frac{1}{\Omega_3^2}\Omega^5 + \left(1 + 2\frac{\Omega_1}{\Omega_3}\right)\Omega^3 - 2\Lambda\Omega^2 + (\omega_0^2 + \Omega_1^2 + \Lambda^2)\Omega - \omega_0^2\Lambda = 0. \quad (40)$$

The notation is introduced: $\Omega = i\omega + \lambda, \omega_0^2 = \kappa/\mu$. The general solution of this equation looks too cumbersome. But to get an idea of the nature of

Table 1
The potential energy parameters of the vortex and inhomogeneity interaction.

Inhomogeneity type	The equilibrium position, ρ_0	Effective stiffness coefficient of the core-defect coupling, κ
Boundary between phases with different magnetic characteristics	$1+\ln\left(\frac{1.7\mu_0 h^2(M_{S1}-M_{S2})^2}{\pi F_x}\right)$	$2F_x/\delta$
The linear inhomogeneity of the bi-directional magnetic anisotropy	$\rho_0 = 0$, for $\alpha\to\pi/2$ or $m_z\to 1$	$\frac{\sqrt{2\pi}}{\delta}Khb\sin^2(\alpha)\left(e^{-2\left(\frac{\delta}{\delta_0}\right)^2}+\frac{\sqrt{2\pi}\delta}{\delta_0}\mathrm{Erf}\left(\frac{\sqrt{2}\delta}{\delta_0}\right)\right)$
	$\rho_0 \approx \pm 0.652$, for $\alpha\to 0$ or $m_z\to 0$	$7.23\frac{Khb}{\delta}\cos^2(\alpha)$
The linear inhomogeneity of the unidirectional magnetic anisotropy	$\rho_0 = 0$, for $\alpha\to\pi/2$ or $m_z\to 1$	$\frac{p}{\delta}Khb\sin(\alpha)\left(e^{-\left(\frac{\delta}{\delta_0}\right)^2}+\frac{\sqrt{\pi}\delta}{\delta_0}\mathrm{Erf}\left(\frac{\delta}{\delta_0}\right)\right)$
	$\rho_0 \approx 0.552$, for $\alpha\to 0$ or $m_z\to 0$	$6.25\frac{qKhb}{\delta}\cos(\alpha)$

the vortex core motion (mode frequencies), a simple special case $D = 0$ (no effective friction) can be considered. In this approximation, after the trivial solution $\Omega = 0$ is eliminated, Eq. (40) takes the form:

$$\frac{1}{\Omega_3^2}\Omega^4+\left(1+2\frac{\Omega_1}{\Omega_3}\right)\Omega^2+\left(\omega_0^2+\Omega_1^2\right)=0. \tag{41}$$

The solution to this biquadrate equation is the expression for ω:

$$\omega^2=\frac{\Omega_3^2}{4}\left(1\mp\sqrt{1+4\frac{\Omega_1}{\Omega_3}-4\frac{\omega_0^2}{\Omega_3^2}}\right)^2+\omega_0^2. \tag{42}$$

In this case ($D\to 0$) we get a frequency doublet. It can be seen from expression (42) that the frequency of periodic motion resembles the frequency of the translational mode $\omega_0=\sqrt{\kappa/\mu}$ [30,31,33] with an addition which gyroscopic effects are responsible for.

The examples of the general solution of Eq. (40) with dissipation are shown in Fig. 8. Possible ratios between the $\Omega_1, \Omega_3, \omega_0$ parameters are selected according to the results of numerical modeling from [60]. The solutions demonstrate the modes with different values of the λ damping parameter for different modes. It is important to note that one of the solutions of Eq. (40) is a real root with a frequency $\omega = 0$ and a damping parameter, the behavior of which is shown by the $\lambda_3^{(1)}$ and $\lambda_3^{(2)}$ curves in Fig. 8b.

The $\lambda_3^{(1)}(D)$ and $\lambda_3^{(2)}(D)$ dependences are qualitatively similar to the ratio $\lambda = \kappa D/(D^2+G^2)$ obtained for the cases of gyrotropic motion of the vortex core in nanoparticles without the inertial term and the third-order gyrotropic term (for example [23,33]). In this case, the return force has a non-zero component only in the projection on one x-axis, which results in the possibility of translational damping motion of the core under certain initial conditions.

Indeed, as it can be concluded from system (37), the square of the amplitudes ratio of a_x^2/a_y^2 in this mode is a real and negative number, which means a synchronous change in the x and y core coordinates. Other modes are gyrotropic modes of motion with a gradual damping of the amplitude and with the asymptotic arrival of the core in a stationary state with uniform motion along the inhomogeneity at a certain equilibrium distance from it, determined by the formula (39). Some implementations of the core trajectory are shown in Fig. 9. This figure shows cases of actual core capture by inhomogeneity. It can be implemented, for example, in the potential created by the inhomogeneity of the local magnetic anisotropy (see Section 2b). The stable equilibrium position of the core without external forces will be determined by the expressions given in Table 1.

4. Discussion of the results

The inclusion of external factors that ensure the existence of constant forces acting on the core leads to the vortex drift. Moreover, in contrast to the early calculations of various authors without higher-order terms, such a movement cannot be considered progressive. The trajectories have cyclicity features, especially in the initial sections (Fig. 7). In our case, the trajectory is an overlay of periodic damping motion and uniform translational displacement.

The study of magnetic vortex behavior near defects in the magnetic structure presents a practical interest. Theoretical consideration of the core motion in the field of linear inhomogeneity of magnetic parameters allowed us to explain qualitatively some interesting properties of trajectories.

When the inhomogeneity looks like a flat boundary at the junction of two magnets with different characteristics, the force field where the core moves is represented by the approximate formula (7). When crossing the

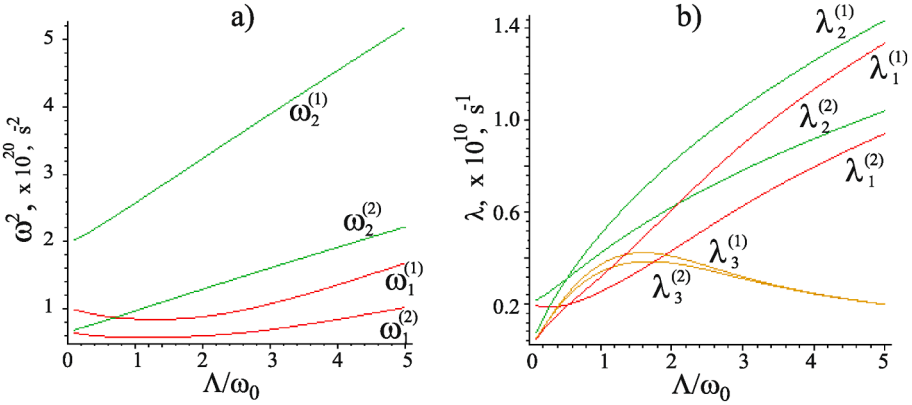

Fig. 8. Imaginary (fig. a) and real (fig. b) parts of the solution of Eq. (40). The curves are constructed for the case $\omega_0 = 10^{10}s^{-1}$, $\Omega_1 = \omega_0$. The lower indices indicate the modes numbers. The upper index "(1) " indicates the curves constructed for $\Omega_3 = \omega_0$, the index "(2)" indicates the curves for $\Omega_3 = 0.5\omega_0$.

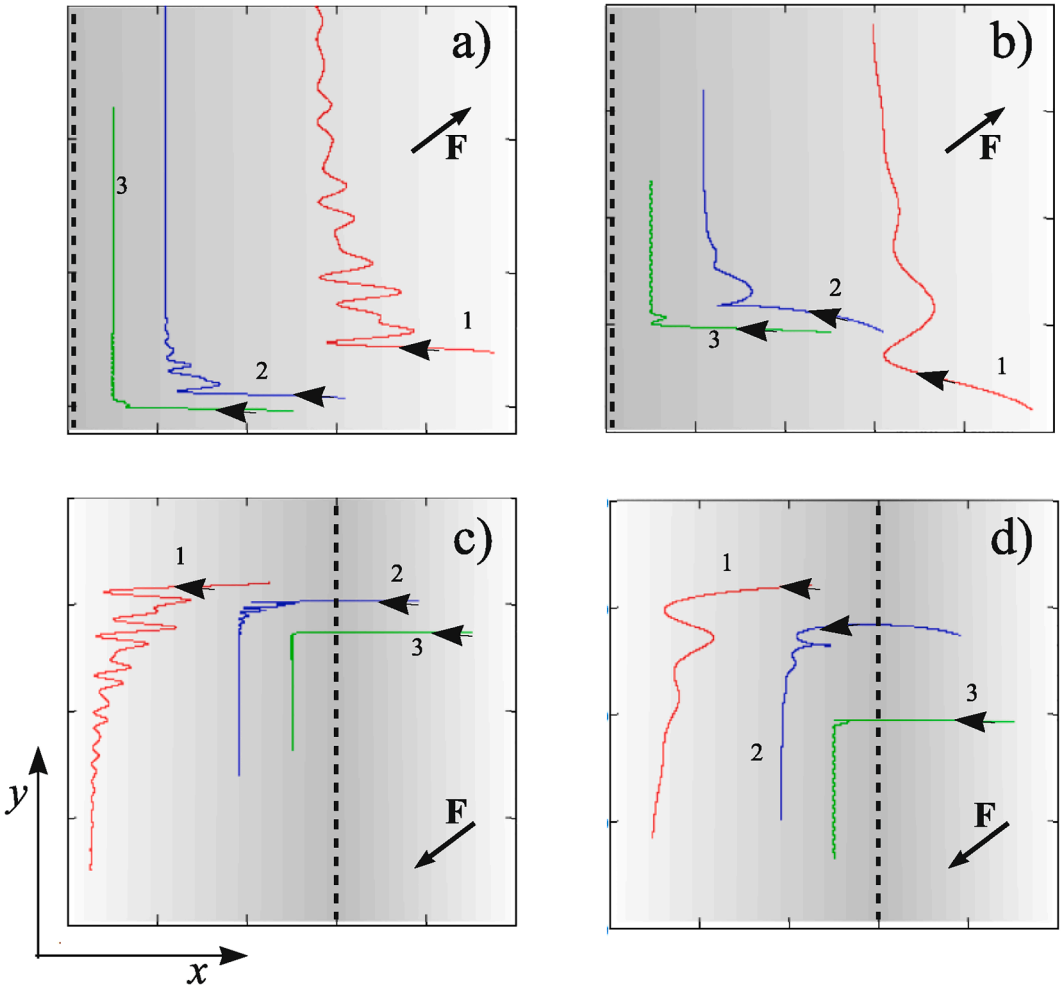

Fig. 9. The trajectories of the magnetic vortex core motion in the field of linear extended inhomogeneity. The position of the minimum energy W is shown by a bold dashed line, a weak gradient fill means the conditional change in the potential created by the inhomogeneity. Curves 1,2,3 are constructed for the cases $\Lambda/\omega_0 = 0.1$, 0.3, 1.0, respectively. The trajectories in figures (a) and (c) are formed under the condition $\Omega_3 = \omega_0$, figures (b) and (d) are influenced by the condition $\Omega_3 = 0.5\omega_0$. The arrows in the corners of the figures show the direction of the constant force **F** acting on the core. The trajectories are constructed for the case of modes superposition in equal parts and $G_1 = \omega_0$.

boundary by means of a jump, all the parameters that characterize the vortex can change: G_3, μ, G, D. It will result in a change of the movement nature. Let's think that the external force acting on the core is directed perpendicular to the boundary ($f_y = 0$). Then it follows from (34) that in the steady motion, the angle of the core incidence on the boundary is approximately equal to $\tan(\phi^{(1)}) = -D^{(1)}/G^{(1)}$. The upper index means the parameters related to the first-class magnet (where the core initially moves). After the core crosses the boundary between the phases, the angle changes: $\tan(\phi^{(2)}) = -D^{(2)}/G^{(2)}$. This phenomenon resemles the light refraction at the boundary of environment with different refractive indices. For the angles ϕ, the expression:

$$\tan\left(\phi\right) = -\frac{D}{G} = -\pi_T \alpha_d \left(1 + \ln\left(\sqrt{\frac{\delta}{\delta_0}}\right)\right). \tag{43}$$

When the core moves to another magnetic phase, the damping parameter and the δ/δ_0 ratio in a general case will change (for example, if the L phase thicknesses differ). But it should be noted that a change in the δ/δ_0 ratio has a weaker effect than a change in the dissipative properties of the environment.

The arguments about ϕ angles are valid at a long distance from the phase boundary and in the case of steady motion. Otherwise, in the field of linear inhomogeneity, the inertial properties and the gyroscopic force of the third order are essential. These factors introduce distortions in the smooth trajectory, causing non-monotonic changes in the components of the core speed and coordinates (for example, Fig. 9 and numerical modeling in [63]).

If the core does not cross the boundary, but there is a repulsive force from it (as in the model discussed in Section 2a or 2b for unidirectional anisotropy), the motion has an interesting feature. Interaction with the inhomogeneity causes a change in the component of the core speed parallel to the boundary. An example of such a movement is shown in Fig. 10. A similar phenomenon was found in numerical modeling presented in the articles [12,47] or theoretical work by [51], where a one-dimensional inhomogeneity was specified by a trigonometric function for example. In these works, the calculations were carried out without the higher-order terms. As a result, smooth trajectories without cyclic features are obtained. In our case, with the $\mathbf{G}_3 \times \ddot{\mathbf{v}}$ and $\hat{\mu}\dot{\mathbf{v}}$ terms, there is also a change in both the x- and y-components of the core speed, but it is not monotonous. The core motion is translational only after the lapse of the $\tau = 1/\lambda$ relaxation time.

Special attention should be paid to the core that moves near a repulsive linear inhomogeneity with the constant external force. We should refer to the formula (39), which determines the equilibrium distance to the inhomogeneity where the core is located after the motion is at a stationary state. It follows from (39) that magnetic vortices (or skyrmions) with different signs of the $\pi_T = pq$ value (opposite signs of the Gparameter) have different equilibrium distances x_0. It makes the

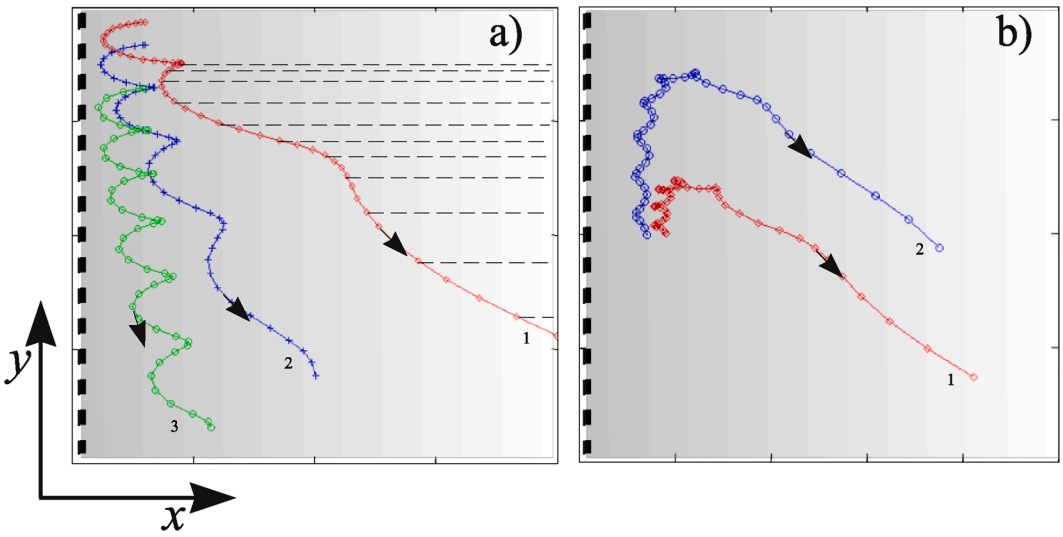

Fig. 10. The example of trajectories obtained as a result of solving the equation of core motion in the field of a repulsive linear defect without external forces. Curves 1,2,3 are obtained at different values of the $\Lambda/\omega_0 = 0.1, 0.05, 0.01$ ratio, respectively. In Fig. (a) at the initial moment of time, the core rates are equal and directed towards the ($v_{0y} = 0$) defect, in Fig. (b) the rates are also equal and directed parallel to the ($v_{0x} = 0$) defect. In Fig. (a), the dotted line means the *y*-coordinates of the core at regular intervals.

gas from the vortices of two varieties with opposite directions of the vector **G**, and hence $\mathbf{G}_3$ under the joint action of an external force and the force created by the inhomogeneity, drift with simultaneous splitting of the trajectories on the sign of the π_T value. In the case of inhomogeneities of local anisotropy, this effect is supplemented by the fact that the force acting on the core from the defect side also depends on the polarity and chirality. Examples of trajectories obtained by solving Eq. (40) are shown in Fig. 11.

Speaking about the motion of cores in ferromagnetic nanoribbons, this phenomenon is called the "skyrmion Hall effect". Modeling the skyrmion motion in nanoribbons without $\mathbf{G}_3$ and $\widehat{\mu}$ allowed us to observe this phenomenon and, of course, the predicted trajectories had smoothness (translational motion) [7,64–66]. The detection of such modes is possible indirectly, for example, in experiments on ferromagnetic resonance.

5. Conclusion

In this paper, we have consider the motions of the magnetic vortex core based on the ideology of collective variables (Thiel's equation), with the dissipative term, the inertial one, and the third-order gyroscopic force. Theoretical analysis has shown a variety of scenarios for the behavior of magnetization near the defect, modeled by an extended linear inhomogeneity of magnetic parameters.

The solution of the equation of motion allowed us to analyze the influence of the inertial term and the gyroscopic term of the third order on the nature of the core motion. The general conclusion about this influence is presented in the following theses.

1. Even in a homogeneous magnetic medium (without fluctuations in the magnetic parameters), the nature of the motion of the magnetic vortex is not translational, but represents some decaying cycloids.
2. The sections of the trajectory of the core corresponding to the beginning of movement, before the steady-state mode of movement,

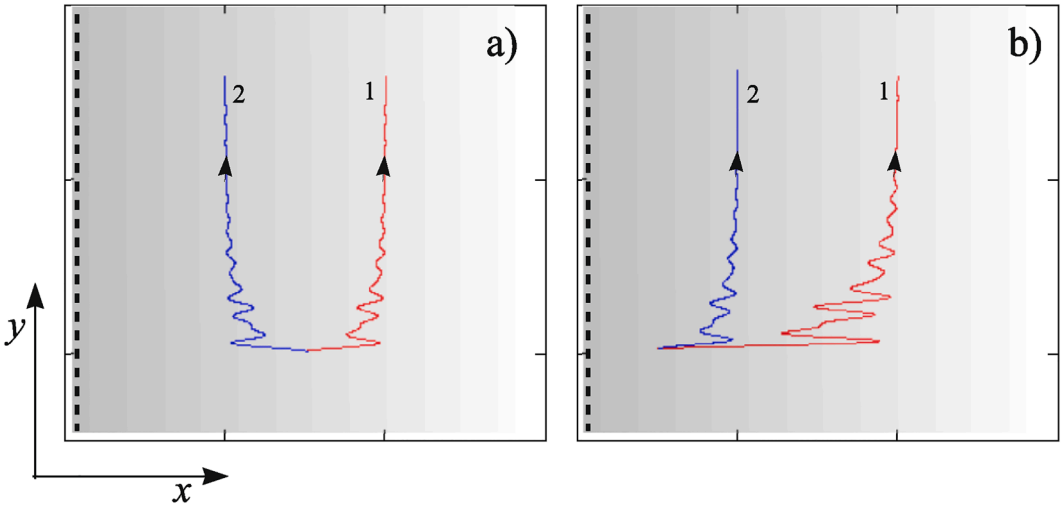

Fig. 11. The example of a vortex trajectory with opposite sign values of the π_T parameters. Curve 1 is made for $\pi_T > 0$, curve 2 is made for $\pi_T < 0$. The trajectories are constructed for the $\Lambda/\omega_0 = 0.15$. relation. The images in figure (a) and (b) differ only in the initial positions of the pair of vortices. The position corresponding to the minimum potential energy is indicated by a dash-dotted line.

have a complex oscillatory character. This circumstance should be noted when designing spintronics devices, which involve controlling the movement of skyrmions by fields and/or spin-polarized currents.

In addition, the process of vortex transition between magnetic phases with different parameters has been considered. The analysis showed that the phenomenon of refraction of the trajectory is observed at the boundary, the angles of incidence and refraction depend on the ratio of the damping parameters in magnetics media.

It is shown that vortices with different sign values of the product of polarity and chirality in the steady-state mode move at different distances from the linear defect. This effect can exist not only because of the difference in the potential energies of vortices with different values of polarities and chiralities (see Section 2), but also because of the sensitivity of the equilibrium distance from the core to the inhomogeneity on the magnitude of external forces. This will allow the selection of cores in the skyrmion gas based on the direction of the **G** and $\mathbf{G}_3$ vectors.

As intermediate results, model expressions have been obtained for the potentials of linear inhomogeneities in the form of the boundary of different magnetic phases and thin inhomogeneities with bidirectional and unidirectional magnetic anisotropy that differs from the main matrix.

Declaration of Competing Interest

The authors declare that they have no known competing financial interests or personal relationships that could have appeared to influence the work reported in this paper.

Acknowledgement

The study has been carried out within the framework of the state task of the Ministry of science and higher education of the Russian Federation (topic No. FSRZ-2020-0011)

References

[1] I. Medlej, A. Hamadeh, F.E.H. Hassan, Physica B: Phys. Condensed Matter 579 (2020), 411900.
[2] M. Chauwin, X. Hu, F. Garcia-Sanchez, N. Betrabet, A. Paler, C. Moutafis, J. S. Friedman, Phys. Rev. App. 12 (2019), 064053.
[3] K.A. Omari, T.J. Hayward, Phys. Rev. App. 2 (2014), 044001.
[4] X. Zhang, M. Ezawa, Y. Zhou, Sci. Rep. 5 (2015) 9400, https://doi.org/10.1038/srep09400.
[5] Sh. Luo, M. Song, X. Li, Y. Zhang, J. Hong, X. Yang, X. Zou, N. Xu, L. You, Nano Lett. 18 (2) (2018) 1180–1184, https://doi.org/10.1021/acs.nanolett.7b04722.
[6] A. Fert, N. Reyren, V. Cros, Nature Rev., Mater. 2, 17031 (2017) 1.
[7] W. Kang, B. Wu, X. Chen, D. Zhu, Zh. Wang, X. Zhang, Y. Zhou, Y. Zhang, W. Zhao. J. Emerg. Technol. Comput. Syst. 16, 1, Article 2 (October 2019), 17 pages.
[8] A.E. Ekomasov, S.V. Stepanov, K.A. Zvezdin, E.G. Ekomasov, J. Magn. Magn. Mater. 471 (2019) 513–520.
[9] Jan Muller, New J. Phys. 19 (2017), 025002.
[10] Y. Zhou, R. Mansell, S. van Dijken, Sci. Rep. 9 6525 (2019) https://doi.org/10.1038/s41598-019-42929-w.
[11] S. Finizio, S. Wintz, E. Kirk, A.K. Suszka, S. Gliga, P. Wohlhuter, K. Zeissler, J. Raabe, Phys. Rev. B 96 (2017), 054438.
[12] Y. Liu, X. Huo, S. Xuan, H. Yan, J. Magn. Magn. Mater. 492 (2019), 165659.
[13] J. Castell-Queralt, L. Gonzalez-Gmez, N. Del-Valle, C. Navau, Phys. Rev. B 101 (2020) 140404(R).
[14] H. Fangohr, S.J. Cox, P.A.J. de Groot, Phys. Rev. B 64 (2001), 064505.
[15] N.P. Vizarim, C.J.O. Reichhardt, P.A. Venegas, C. Reichhardt, Eur. Phys. J. B 93 (2020) 112.
[16] W. Chen, L. Liu, Y. Zheng, Phys. Rev. App. 14 (2020), 064014.
[17] Stosic Dusan, Numerical simulations of magnetic skyrmions in atomically-thin ferromagnetic films/Dusan Stosic, Universidade Federal de Pernambuco (2018) 149.
[18] N.A. Usov, S.E. Peschany, J. Magn. Magn. Mater. 118 (1993) L290–L294.
[19] W. Scholz, K.Yu. Guslienko, V. Novosad, D. Suess, T. Schrefl, R.W. Chantrell, J. Fidler, J. Magn. Magn. Mater. 266 (2003) 1551163.
[20] A.A. Thiele, J. of Appl. Phys. 45 (1) (1974) 377–393.
[21] A.R. Volkel, G.M. Wysin, F.G. Mertens, A.R. Bishop, H.J. Schnitzer, Phys. Rev. B 50 (17) (1994) 12711–12720.
[22] B.A. Ivanov, H.J. Schnitzer, F.G. Mertens, G.M. Wysin, Phys. Rev. B 58 (1998) 8464–8474.
[23] J. Kim, S.-B. Choe, J. Magn. 12 (3) (2007) 113.
[24] A.K. Zvezdin, K.A. Zvezdin, J. Low Temp. Phys. 36 (2010) 826.
[25] B.A. Ivanov, G.G. Avanesyan, A.V. Khvalkovskiy, N.E. Kulagin, C.E. Zaspel, K. A. Zvezdin, JETP Lett. 91 (2010) 178–182.
[26] K.Yu. Guslienko, B.A. Ivanov, V. Novosad, Y. Otani, H. Shima, K. Fukamichi, J. Appl. Phys. 91 (2002) 8037.
[27] G.M. Wysin, F.G. Mertens, A.R. Völkel, A.R. Bishop, Nonlinear Coherent Structures in Physics and Biology, edited by K.H. Spatschek and F.G. Mertens (Plenum, New York, 1994).
[28] F.G. Mertens, H.J. Schnitzer, A.R. Bishop, Phys. Rev. B 56 (5) (1997) 2510–2520.
[29] D.A. Carvajal, A. Riveros, J. Escrig, Results Phys. 19 (2020), 103598.
[30] Y.-F. Chen, Z.-X. Li, Z.-W. Zhou, Q.-L. Xia, Y.-Z. Nie, G.-H. Guo, J. Magn. Magn. Mater. 458 (2018) 123–128.
[31] G.M. Wysin, Phys. Rev. B 54 (21) (1996) 15156–15162.
[32] D. Reitz, A. Ghosh, O. Tchernyshyov, Phys. Rev. B 97 (2018), 054424.
[33] P.D. Kim, V.A. Orlov, V.S. Prokopenko, S.S. Zamai, V.Ya. Prints, R.Yu. Rudenko, T. V. Rudenko, Phys. Solid State 57 (2015) 30–37.
[34] K.Y. Guslienko, R. Hernandez, O. Chubykalo-Fesenko, Phys. Rev. B 82 (2010), 014402.
[35] J. Muller, A. Rosch, Phys. Rev. B 91 (2015), 054410.
[36] C.C.I. Ang, W. Gan, W.S. Lew, New J. Phys. 21 (2019), 043006.
[37] R. Tomasello, S. Komineas, G. Siracusano, M. Carpentieri, G. Finocchio, Phys. Rev. B 98 (2018), 024421.
[38] H.T. Fook, W.L. Gan, W.S. Lew, Sci. Rep. 6 (2016) 21099, https://doi.org/10.1038/srep21099.
[39] X. Liang, G. Zhao, L. Shen, J. Xia, L. Zhao, X. Zhang, Y. Zhou, Phys. Rev. B 100 (2019), 144439.
[40] M. Rahma, J. Biberger, V. Umansky, D. Weiss, J. Appl. Phys. 93 (2003) 7429.
[41] Ch. Hanneken, A. Kubetzka, K. von Bergmann, R. Wiesendanger, New J. Phys. 18 (2016), 055009.
[42] R.L. Compton, P.A. Crowell, Phys. Rev. Lett. 97 (2006), 137202.
[43] C. Navau, N. Del-Valle, A. Sanchez, J. Magn. Magn. Mater. 465 (2018) 709–715.
[44] C. Song, C. Jin, H. Xia, Y. Ma, J. Wang, J. Wang, Q. Liu, arXiv:2005.03385v2 [cond-mat.mes-hall] 8 May (2020).
[45] A. Derras-Chouk, E.M. Chudnovsky, arXiv:2010.14683v1 [cond-mat.mes-hall] 28 Oct (2020).
[46] V.A. Orlov, G.S. Patrin, I.N. Orlova, J. Exp. Theor. Phys. 131 (2020) 589–599.
[47] J. Castell-Queralt, L. Gonzalez-Gmez, N. Del-Valle, A. Sanchez, C. Navau, Nanoscale 11 (2019) 12589.
[48] C. Reichhardt, D. Ray, C.J. Olson Reichhardt, Phys. Rev. Lett. 114 (2015), 217202.
[49] Mertens F.G., Bishop A.R. Dynamics of Vortices in Two-Dimensional Magnets. In: Christiansen P.L., Soerensen M.P., Scott A.C. (eds) Nonlinear Science at the Dawn of the 21st Century. Lecture Notes in Physics, vol 542. Springer, Berlin, Heidelberg (2000). (https://doi.org/10.1007/3-540-46629-0-7).
[50] S.K. Kim, Y. Tserkovnyak, Appl. Phys. Lett. 111 (2017), 032401 (https://doi.org/10.1063/1.4985577).
[51] J.C. Martinez, M.B.A. Jalil, J. Magn. Magn. Mater. 424 (2017) 291–297, https://doi.org/10.1016/j.jmmm.2016.10.026.
[52] J.P. Park, P. Eames, D.M. Engebretson, J. Berezovsky, P.A. Crowell, Phys. Rev. B 67 (2003) 020403(R), https://doi.org/10.1103/PhysRevB.67.020403.
[53] J. Park, P.A. Crowell, Phys. Rev. Lett. 95 (2005), 167201, https://doi.org/10.1103/PhysRevLett.95.167201.
[54] X. Zhu, Zh. Liu, V. Metlushko, P. Grutter, M.R. Freeman, Phys. Rev. B 71 (2005) 1804089(R), https://doi.org/10.1103/PhysRevB.71.18040.
[55] B.A. Ivanov, C.E. Zaspel, Phys. Rew. Lett. 99 (2007), 247208.
[56] K.Yu. Guslienko, Appl. Phys. Lett. 89 (2006), 022510.
[57] A.K. Zvezdin, V.I. Belotelov, K.A. Zvezdin, JETP Lett. 87 (7) (2008) 381–384.
[58] V.P. Kravchuk, D.D. Sheka, U.K. Robler, J. van den Brink, Y. Gaididei, Phys. Rev. B 97 (2018), 064403.
[59] I. Makhfudz, B. Kruger, O. Tchernyshyov, Phys. Rev. Lett. 109 (2012), 217201.
[60] Z.-X. Li, C. Wang, Y. Cao, P. Yan, Phys. Rev. B 98 (2018) 180407R.
[61] Y. Liu, Z. Liang, J. Magn. Magn. Mater. 500 (2020), 166382.
[62] K.Y. Guslienko, G.N. Kakazei, J. Ding, X.M. Liu, A.O. Adeyeye, Sci. Rep. 5 (2015) 13881, https://doi.org/10.1038/srep13881.
[63] J. Wang, J. Xia, X. Zhang, X. Zheng, G. Li, Y. Li Chen, J. Zhou, H. Wu, R. Yin, Y. Xu. Chantrell, Appl. Phys. Lett. 117 (2020), 202401.
[64] J.-Y. Lee, K.-S. Lee, S. Choi, K.Y. Guslienko, S.-K. Kim, Phys. Rev. B 76 (2007), 184408.
[65] K.Yu. Guslienko, J.-Y. Lee, S.-K. Kim, IEEE Trans. On Magn. 44 (11) (2008) 3079.
[66] X. Xing, J. Ekerman, Y. Zhou, Phys. Rev. B 101 (2020), 214432.